tabase for Mean Monthly Values of Temperature, Precipitation & Cloudiness on a Terrestrial Grid (International Institute for Applied Systems Analysis, Laxenburg, Germany, 1991).
21. J. Lloyd and G. D. Farquhar, *Oecologia* **99**, 201 (1994).
22. I. C. Prentice *et al.*, *J. Biogeogr.* **19**, 117 (1992).
23. A preindustrial atmospheric CO_2 concentration of 280 ppmv was used [G. I. Pearman *et al.*, *Nature* **320**, 248 (1986); A. Neftel *et al.*, *ibid.* **331**, 609 (1988)].
24. J. F. Griffiths, *Climate of Africa* (Elsevier, Amsterdam, 1972).
25. O. Hedberg, *Sven. Bot. Tidskr.* **45**, 141 (1951).
26. A. C. Hamilton, *Palaeoecol. Afr.* **7**, 45 (1972); E. M. Van Zinderen Bakker, *ibid.* **14**, 77 (1982). Recent pollen analyses from lowland Amazonia have suggested an LGM temperature on the same order of 5° to 6°C [P. A. Colinvaux, P. E. De Oliveira, J. E. Moreno, M. C. Miller, M. B. Bush, *Science* **274**, 85 (1996)].
27. I. Terashima *et al.*, *Ecology* **76**, 2663 (1995).
28. D. Taylor, *Palaeogeogr. Palaeoclimatol. Palaeoecol.* **80**, 283 (1990).
29. W. Dansgaard *et al.*, *Nature* **364**, 218 (1993); G. Bond *et al.*, *ibid.* **365**, 143 (1993).
30. CLIMAP Project Members, *Geol. Soc. Am. Map Chart Ser. MC-36* (1981); D. Rind and D. Peteet, *Quat. Res.* **24**, 1 (1985).
31. Supported by the Swedish Natural Science Research Council (NFR) and by the U.S. Environmental Protection Agency under a subcontract with the University of New Hampshire in support of International Geosphere-Biosphere Program (IGBP) GAIM activities. This is a contribution to the (NSF) TEMPO, (European Union) PMIP, RUKWA, and (PNEDC) ERICA projects and to the core research of IGBP-GCTE. We thank I. C. Prentice and two anonymous reviewers for comments on the manuscript.

2 December 1996; accepted 10 March 1997

Surface Deformation and Lower Crustal Flow in Eastern Tibet

Leigh H. Royden,* B. Clark Burchfiel, Robert W. King, Erchie Wang, Zhiliang Chen, Feng Shen, Yuping Liu

Field observations and satellite geodesy indicate that little crustal shortening has occurred along the central to southern margin of the eastern Tibetan plateau since about 4 million years ago. Instead, central eastern Tibet has been nearly stationary relative to southeastern China, southeastern Tibet has rotated clockwise without major crustal shortening, and the crust along portions of the eastern plateau margin has been extended. Modeling suggests that these phenomena are the result of continental convergence where the lower crust is so weak that upper crustal deformation is decoupled from the motion of the underlying mantle. This model also predicts east-west extension on the high plateau without convective removal of Tibetan lithosphere and without eastward movement of the crust east of the plateau.

The topography and geology of the Tibetan region resulted from postcollision north-south convergence between the Indian and Eurasian plates since ~50 million years ago (Ma) (*1–3*) (Fig. 1). In this process, the Tibetan plateau was uplifted by >4 km and its crust thickened to twice normal thickness (~70 km) (*4–10*). Several competing models have been proposed for the uplift and deformation of Tibet, each with different implications for the eastern part of the Tibetan plateau (*11–17*). Here, we propose a model for the crustal dynamics within the plateau on the basis of geologic and Global Positioning System (GPS) observations of young crustal deformation along the eastern margin of the plateau.

Much of the eastern margin of the plateau lacks evidence for large-scale young crustal shortening; folds and thrust faults along the plateau margin are commonly oblique to and older than the plateau margin (*18*). In the Northern Longmen Shan, folds and faults trend east-west, nearly perpendicular to the plateau edge, and are mainly of Mesozoic age. In the south central Longmen Shan, the crust was probably shortened by ~100 km in Mio-Pliocene time, but there is no evidence for major Quaternary shortening. GPS results are consistent and constrain shortening across the Longmen Shan to be 0 ± 5 mm year^{-1} (*19, 20*). This lack of young deformation is surprising because the topographic front of the eastern plateau is as impressive as that of the Himalayas.

A similar mismatch between surface structure and topography occurs in the Yunnan region (south of the Xianshuihe fault). The active faults in this region cross from the high plateau into regions of lower elevation in southeast China (*19*). They are predominantly left-slip and trend south to southeast, nearly perpendicular to the plateau margin (Fig. 1B). Both geological and GPS results indicate slip on the Xianshuihe fault at ~20 mm year^{-1} (*19–21*). However, since 4 Ma or earlier, the southeastern corner of the plateau has rotated clockwise around the eastern Himalayan syntaxis with little, if any, net translation of upper crustal material eastward across or into the plateau margin (*19*). Thus, although we cannot rule out the possibility of eastward extrusion of Tibetan crust relative to Siberia in Pliocene-Quaternary time, there are no data to support this hypothesis, and, if extrusion occurs, southern China must be moving eastward at approximately the same rate as the central and southern parts of eastern Tibet.

Also noteworthy is the lack of a Cenozoic foredeep basin along the eastern margin of the plateau, which implies that the eastern foreland was not flexurally depressed during Cenozoic time. [Although the Sichuan basin is often considered to be a foredeep basin to the eastern plateau, rocks exposed in the basin are mainly Mesozoic in age. Where present, the Cenozoic cover is thin (≤200 m), and pre–Late Quaternary rocks are eroding throughout most of the Sichuan basin (*18*)]. A zone of extensional structures formed by margin-perpendicular extension of unknown Cenozoic age coincides with the topographically high mountains that rim the edge of the eastern plateau (*18*). These structures are reminiscent of the low-angle normal faults present along the northern margin of the Himalayas (*22*).

Various models of Cenozoic deformation within Tibet indicate that the uplift and surface deformation of the Tibetan plateau are intimately linked to the manner in which the crust beneath the plateau has been deformed at depth (*14, 15, 23–25*). However, these models do not match the observed surface deformation of Tibet in a number of important ways (*26*): They do not display east-west extension or eastward motions of the plateau (*26, 27*), they do not display large clockwise rotation of crustal material around the eastern Himalayan syntaxis (*19–21*), they do not reproduce margin-parallel extension along the plateau margin (*18*), and they do not offer a satisfactory explanation for the lack of surface shortening along the southeastern margin of the plateau (*18, 19*).

In two dimensions, quantitative studies of model convergent systems have shown that topography, strain partitioning, and degree of crust-mantle coupling are systematically related to the strength (viscosity) of the crust as a function of increasing depth (*25, 28, 29*). In particular, steep-sided flat-topped plateaus develop only when a low-viscosity zone is absent beneath the foreland and the margins of the plateau but is present in regions of thickened crust beneath the plateau proper. Because recent studies suggest that the lower crust beneath Tibet may be weak (*30, 31*), some of the inadequacies in the thin viscous sheet models may occur because such models ignore depth-dependent behavior and thus cannot incorporate lateral shear

L. H. Royden, B. C. Burchfiel, R. W. King, E. Wang, Department of Earth, Atmospheric, and Planetary Sciences, Massachusetts Institute of Technology, Cambridge, MA 02139, USA.
Z. Chen, F. Shen, Y. Liu, Chengdu Institute of Geology and Mineral Resources, Chengdu, China.
*To whom correspondence should be addressed.

between the upper crust and the lower crust and mantle. We explored the effects of incorporating depth-dependent rheologies into geodynamic models of plateau formation by means of an analytic solution for three-dimensional basally driven deformation in an idealized crust with depth-dependent Newtonian viscosity. We assumed that the mantle lithosphere behaves in a plate-like fashion and that each of two mantle plates is translated toward a narrow mantle suture at a uniform and constant rate. The horizontal velocity at the base of the crust was set equal to the velocity of the underlying mantle. Crustal viscosity was a function only of depth (relative to the topographic surface) and was laterally invariant. We used a viscosity-depth function that produced a plateau with about the same width, height, and marginal slope as the Tibetan plateau (*28*, *32*, *33*) and all topography was locally compensated.

The morphology of the plateau produced by the model looks similar to that of the current eastern half of the Tibetan plateau after 40 million years (My) of convergence (Figs. 1A and 2A). In the model, rapid shortening of the upper crust occurs along the southern, northern, northwestern, and northeastern margins of the plateau, and slow shortening of the upper crust occurs along the southeastern and southwestern plateau margins. The model also showed slow east-west extension (at 10 to 20 mm year^{-1} for a total extensional strain of ~30%) and slow north-south shortening of the upper crust, distributed uniformly across the plateau proper, as well as localized extension at the edges of the high plateau. Thus, convective removal of Tibetan mantle lithosphere (*24*) is not necessary to explain the observed east-west extension of the Tibetan plateau.

In the model, a high region developed south and east of the eastern Himalayan syntaxis. This high area formed during convergence as material flowed eastward and southward away from the high plateau. Model deformation in this region consisted largely of clockwise rotations of material around the eastern syntaxis, with surface velocities as high as 15 mm year^{-1} in a south to southeast direction relative to the eastern foreland (Fig. 2A). Cumulative deformation of an originally orthogonal surface mesh shows that the crust has been rotated clockwise by >180° around the eastern syntaxis (Fig. 2B). A broadly distributed north-trending zone of right shear has affected the crust in the southeastern plateau, but this zone disappears northward as shear is absorbed by the rotation of crustal material around the syntaxis. In the model, this zone of right shear is partly coincident with a zone of extension, with the magnitude of extension very large near the syntaxis.

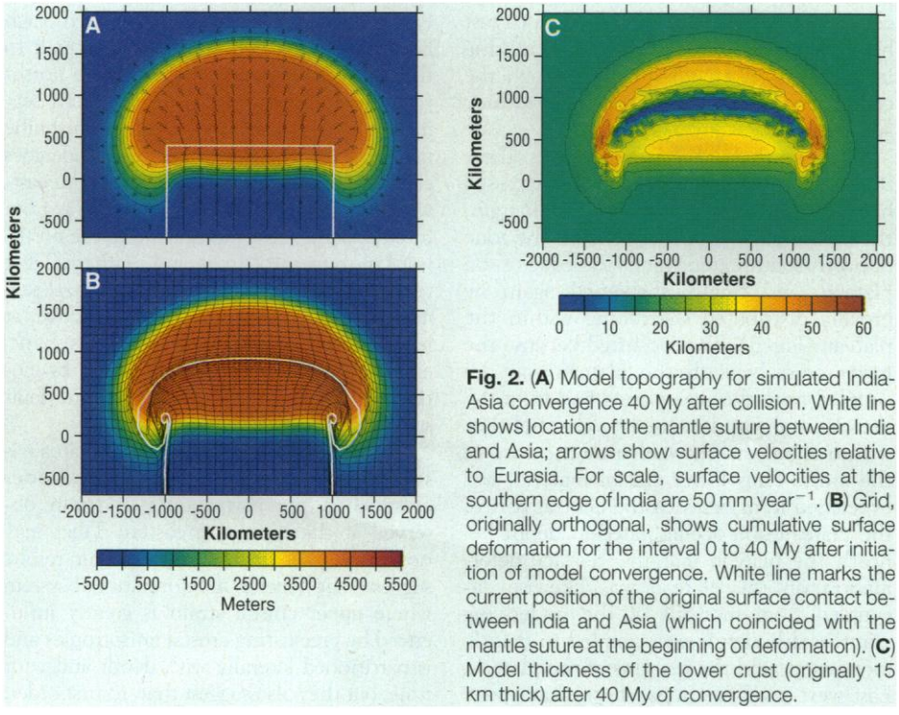

Fig. 2. (**A**) Model topography for simulated India-Asia convergence 40 My after collision. White line shows location of the mantle suture between India and Asia; arrows show surface velocities relative to Eurasia. For scale, surface velocities at the southern edge of India are 50 mm year^{-1}. (**B**) Grid, originally orthogonal, shows cumulative surface deformation for the interval 0 to 40 My after initiation of model convergence. White line marks the current position of the original surface contact between India and Asia (which coincided with the mantle suture at the beginning of deformation). (**C**) Model thickness of the lower crust (originally 15 km thick) after 40 My of convergence.

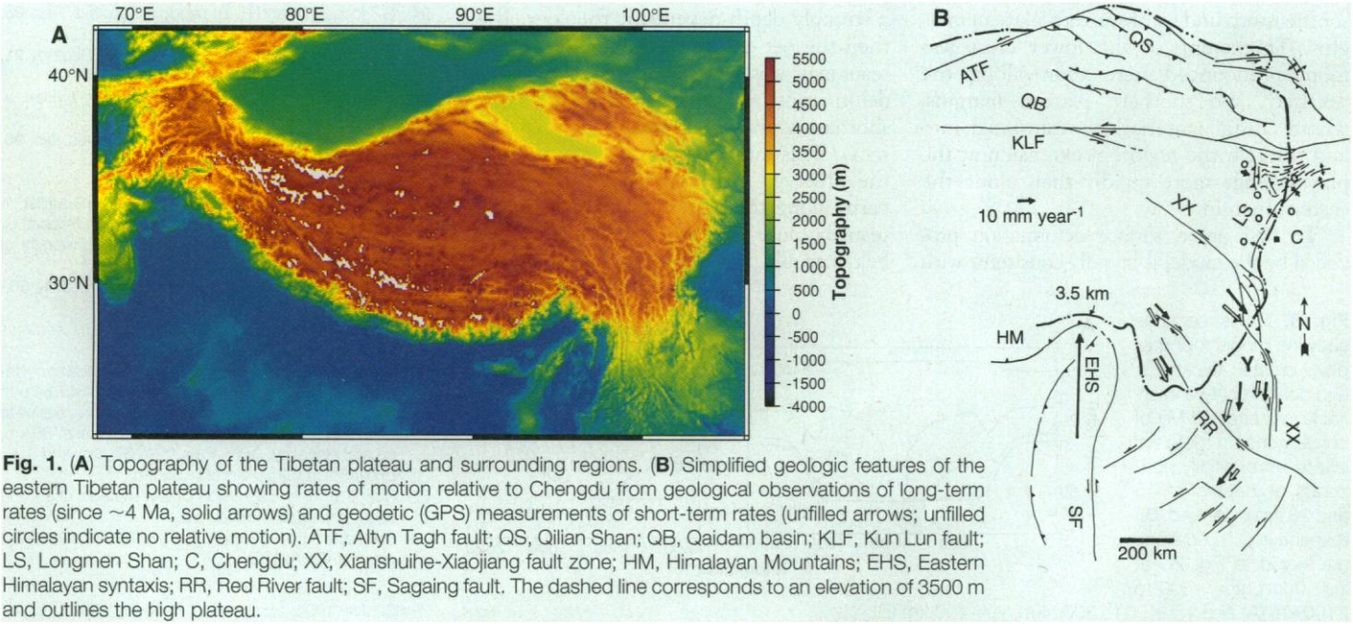

Fig. 1. (**A**) Topography of the Tibetan plateau and surrounding regions. (**B**) Simplified geologic features of the eastern Tibetan plateau showing rates of motion relative to Chengdu from geological observations of long-term rates (since ~4 Ma, solid arrows) and geodetic (GPS) measurements of short-term rates (unfilled arrows; unfilled circles indicate no relative motion). ATF, Altyn Tagh fault; QS, Qilian Shan; QB, Qaidam basin; KLF, Kun Lun fault; LS, Longmen Shan; C, Chengdu; XX, Xianshuihe-Xiaojiang fault zone; HM, Himalayan Mountains; EHS, Eastern Himalayan syntaxis; RR, Red River fault; SF, Sagaing fault. The dashed line corresponds to an elevation of 3500 m and outlines the high plateau.

Despite the regularity of the total crustal thickness in the model (which was linearly proportional to local topographic elevation), the thicknesses of the upper and lower crust were highly variable (Fig. 2C). In the model, the upper crust (defined as that part of the crust corresponding to the upper 15 km of crust before convergence) was thickened to ~30 km across most of the plateau, but it was ~60 km thick in an east-west–trending zone through the center of the plateau and was thin (~5 km) adjacent to the eastern and western syntaxis. Correspondingly, the lower crust (defined as that part of the crust corresponding to the lower 15 km of crust before convergence) was essentially missing in an east-west–trending zone through the center of the plateau but was very thick adjacent to the eastern syntaxis.

The north-south cross sections show that the upper crust thickened as it passed beneath the foot of the plateau margin, then thinned as it passed beneath the zone of north-south extension at the edge of the plateau, and finally thickened again by broadly distributed shortening within the plateau (Fig. 3). This occurred because the lower crust beneath the plateau was decoupled from the upper crust and from the mantle, and was deformed by channel flow within a narrow channel near the base of the crust. Thus lower crustal material was evacuated from beneath the central part of the plateau and accumulated at depth beneath the plateau margins. Surface deformation on the plateau was likewise decoupled from motions of the underlying mantle, although it was coupled to mantle motions around the margins of the plateau. East-west cross sections show that lower crustal rocks were thickened and upper crustal rocks were thinned adjacent to the southeastern and southwestern plateau margins. Thickening of the lower crust was more pronounced here than along the northern and southern plateau margins, where crustal material was translated into and through the region of extension at the plateau edge more rapidly than along the eastern margin.

To first order, surface deformation produced by the model is broadly consistent with the observed deformation in eastern Tibet. The primary difference is that the observed deformation is strongly partitioned by active left-slip fault zones that follow older crustal anisotropies (5). Our results suggest that strain partitioning may be a secondary feature resulting from lateral inhomogeneities in crustal strength. Thus, a possible interpretation of the young surface deformation in central to eastern Tibet can be obtained by combining the observed deformation in Tibet with the surface velocity field derived from our model results [see also (27)]. In this interpretation, the northern segment of the eastern plateau (Qilian Shan), bounded by the Altyn Tagh fault to the north and the Kun Lun fault to the south, is dominated by north- to northeast-directed shortening. The southern segment (Yunnan), bounded by the Xianshuihe fault zone to the north and east, undergoes clockwise rotation that is related to the eastward movement of crustal material away from internal parts of the plateau and to the northward movement of India and southern Tibet relative to southeast China. The central segment (Longmen Shan) is largely inactive, at least at the surface, and active strain is shunted around the Longmen Shan region by motion on the Kun Lun and Xianshuihe fault systems.

If surface deformation on the plateau is strongly decoupled from motion of the lower crust, then the partitioning of strain observed at the surface in eastern Tibet may not extend to the lower crust. Our results suggest that Tibet is a deformational system where upper crustal strain is greatly influenced by preexisting crustal anisotropies and is partitioned laterally with depth and with time, but they also suggest that, to first order, the deformation of Tibet can be understood as deformation of a continuous medium with a strongly depth-dependent rheology. If so, then the net crustal thickening on the plateau may not correspond to upper crustal deformation and may occur by differential shortening and thickening of lower crustal rocks. This interpretation is consistent with the observed lack of a Cenozoic foredeep basin along the eastern margin of the plateau, because thickening of the crust from below would not cause loading and subsidence of the adjacent foreland if much of the flexural strength of the lithosphere is localized in the upper to middle crust.

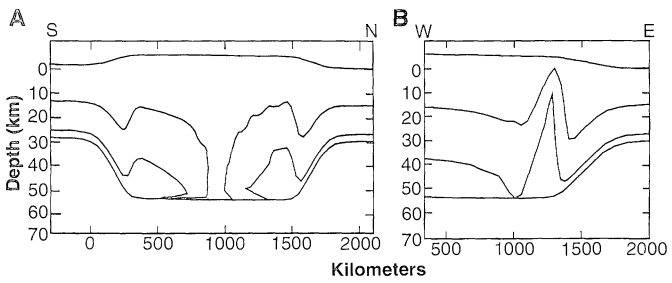

Fig. 3. Cross sections showing model topography, crustal thickness, and position of two internal layers after 40 My of convergence. Internal layers were initially horizontal at depths of 15 and 28 km in (**A**) and (**B**), respectively. Locations are keyed to Fig. 2C at x = 0 km, y = –300 to 2100 km (A) and x = 400 to 2000 km, y = 400 km (B).

REFERENCES AND NOTES

1. P. Molnar and P. Tapponnier, *Science* **189**, 419 (1975).
2. E. Argand, *Proc. 13th Int. Geol. Congr. Brussels* (1924), vol. 1, p. 171.
3. L. Jolivet, P. Davy, P. Cobbold, *Tectonics* **9**, 1409 (1990).
4. P. Molnar, *Philos. Trans. R. Soc. London Ser. A* **326**, 33 (1988).
5. B. C. Burchfiel and L. H. Royden, *Eclogae Geol. Helv.* **84**, 599 (1991).
6. M. P. Coward, W. S. F. Kidd, Y. Pan, R. M. Shackleton, H. Zhang, *Philos. Trans. R. Soc. London Ser. A* **327**, 307 (1988).
7. M. E. Coleman and K. V. Hodges, *Nature* **374**, 49 (1995).
8. T. M. Harrison, P. Copeland, W. S. F. Kidd, A. Yin, *Science* **255**, 1663 (1992).
9. S. C. Turner *et al.*, *Nature* **364**, 50 (1993).
10. R. Xu, in *Geology, Geological History and Origin of Qinghai-Xizang Plateau* (Science Press, Beijing, 1981), vol. 1, pp. 139–144.
11. J. F. Dewey and K. C. A. Burke, *J. Geol.* **81**, 683 (1973).
12. P. Molnar and P. Tapponnier, *Geology* **5**, 212 (1977).
13. P. Tapponnier, G. Peltzer, A. Y. Le Dain, R. Armijo, P. Cobbold, *ibid.* **10**, 611 (1982).
14. P. C. England and G. A. Houseman, *J. Geophys. Res.* **91**, 3664 (1986).
15. ———, *Philos. Trans. R. Soc. London Ser. A* **326**, 301 (1988).
16. W. L. Zhao and W. J. Morgan, *Tectonics* **4**, 359 (1985).
17. J. P. Avouac and P. Tapponnier, *Geophys. Res. Lett.* **20**, 895 (1993).
18. B. C. Burchfiel, Z. Chen, Y. Liu, L. H. Royden, *Int. Geol. Rev.* **37**, 661 (1995).
19. E. Wang *et al.*, in preparation.
20. F. Shen *et al.*, *Proceedings of the International Union of Geodesy and Geophysics, XXI General Assembly* (Boulder, CO, 2 to 14 July 1995), abstract Week A, p. 29.
21. R. W. King *et al.*, *Geology* **25**, 179 (1997).
22. B. C. Burchfiel *et al.*, *Geol. Soc. Am. Spec. Pap. 269* (1992).
23. P. C. England and D. P. McKenzie, *Geophys. J. R. Astron. Soc.* **70**, 295 (1982).
24. G. Houseman and P. England, *J. Geophys. Res.* **98**, 12233 (1993).
25. S. D. Willet, C. Beaumont, P. Fullsack, *Geology* **21**, 371 (1993).
26. R. Armijo, P. Tapponnier, J. L. Mercier, T. Han, *J. Geophys. Res.* **91**, 13803 (1986).
27. W. E. Holt, J. F. Ni, T. C. Wallace, A. Haines, *ibid.* **96**, 14595 (1991).
28. L. H. Royden, *ibid.* **101**, 17679 (1996).
29. C. Beaumont, P. Fullsack, J. Hamilton, S. Willet, in *Alberta Basement Transects, Workshop Report*, G. M. Ross, Ed. (Lithoprobe Secretariat, University of British Columbia, 1992), vol. 228, p. 22.
30. Y. Jin, M. McNutt, Z. Yongshen, *Nature* **371**, 669 (1994).
31. J. G. Masek, B. L. Isacks, E. J. Fielding, *Tectonics* **13**, 659 (1994).
32. Values used in the calculations are as follows: northward velocity of Indian mantle relative to Asia, 50 mm year^{-1}; northward velocity of mantle suture relative to Asia, 10 mm year^{-1}; initial crustal thickness, 30 km; crustal viscosity, 10^{21} Pa·s (z < 55 km) and 10^{21} exp[(55 – z)/0.25] Pa·s (z > 55 km).
33. See (*28*) for a discussion of the method used and assumptions and limitations.

34. Supported by NSF grant EAR-8904096 and NASA grant NAGW-2155.

22 July 1996; accepted 21 February 1997